Eur. Phys. J. C 52, 571–579 (2007)
DOI 10.1140/epjc/s10052-007-0419-z

THE EUROPEAN PHYSICAL JOURNAL C

Regular Article – Theoretical Physics

x-dependence of the quark distribution functions in the χCQM$_{\text{config}}$

H. Dahiya[a], M. Gupta

Department of Physics, Centre of Advanced Study in Physics, Panjab University, Chandigarh – 160 014, India

Received: 25 July 2007 / Revised version: 31 August 2007 /
Published online: 26 September 2007 –

Abstract. Chiral constituent quark model with configuration mixing (χCQM$_{\text{config}}$) is known to provide a satisfactory explanation of the "proton spin problem" and related issues. In order to enlarge the scope of χCQM$_{\text{config}}$, we have attempted to phenomenologically incorporate x-dependence in the quark distribution functions. In particular, apart from calculating valence and sea quark distributions $q_{\text{val}}(x)$ and $\bar{q}(x)$, we have carried out a detailed analysis to estimate the sea quark asymmetries $\bar{d}(x)-\bar{u}(x)$, $\bar{d}(x)/\bar{u}(x)$ and $\frac{\bar{d}(x)-\bar{u}(x)}{u(x)-d(x)}$ as well as spin independent structure functions $F_2^p(x)-F_2^n(x)$ and $F_2^n(x)/F_2^p(x)$ as functions of x. We are able to achieve a satisfactory fit for all the above mentioned quantities simultaneously. The inclusion of effects due to configuration mixing have also been examined in the case $F_2^p(x)-F_2^n(x)$ and $F_2^n(x)/F_2^p(x)$ where the valence quark distributions dominate and it is found that it leads to considerable improvement in the results. Further, the valence quark structure has also be tested by extrapolating the predictions of our model in the limit $x \to 1$ where data is not available.

1 Introduction

Chiral constituent quark model (χCQM), as formulated by Manohar and Georgi [1,2], has been successful in not only explaining the "proton spin crisis" [3–8] but is also able to account for various general features of the quark flavor and spin distribution functions including the violation of Gottfried sum rule [9–14], baryon magnetic moments and hyperon β-decay parameters etc. [15–22]. Recently, it has been shown that configuration mixing, known to be compatible with the χCQM (henceforth to be referred as χCQM$_{\text{config}}$), improves the predictions of χCQM regarding the spin polarization functions as well as gives an excellent fit to the baryon magnetic moments [23–26]. The successes of χCQM$_{\text{config}}$ have been tested rather well for the quantities which are Q^2 as well as x independent. In this context, it may be added that in the last few years, there has been considerable refinement in the measurements of $\bar{d}-\bar{u}$ and $\bar{d}/\bar{u}$ asymmetry as well as $\frac{\bar{d}-\bar{u}}{u-d}$ at different values of Bjorken scaling variable x. The NuSea Experiment (E866) [11–13] has determined independently how the sea-antiquark ratio $\bar{d}/\bar{u}$ and the difference $\bar{d}-\bar{u}$ vary with x and it has been found that the Q^2 dependence is small in these quantities. Earlier, the NMC data was available for $\bar{d}-\bar{u}$ [9,10] for a range of x and NA51 measurements for $\bar{d}/\bar{u}$ [27] were constrained at a single value of x. More recently, HERMES has presented the x-dependence of another $u-d$ asymmetry $\frac{\bar{d}-\bar{u}}{u-d}$ [28]. This suggests a corresponding extension of the successes of χCQM$_{\text{config}}$ to quantities which are x-dependent but have weak Q^2 dependence.

Similarly, the combinations of proton and neutron structure functions $F_2^{p,n}(x,Q^2)$, having weak dependence on Q^2, provide a good facility to test the quark distribution functions at different x values [29,30]. In particular, the experimental data is available for the difference of proton and neutron structure functions $F_2^p(x)-F_2^n(x)$ as well as the ratio $R^{np}(x)=F_2^n(x)/F_2^p(x)$ [29,30]. It has been emphasized in the literature that they provide vital clues to the valence structure of the nucleons in the limit $x \to 1$ thereby having important implications for the valence quark distribution functions. Also, in this limit, such an exercise has a bearing on the configuration mixing as well [31–39].

It has been emphasized in the neutrino-induced DIS experimental data from the CDHS experiment that, on the one hand, the valence quark distributions dominate for $x > 0.3$ and it is a relatively clean region to test the valence structure of the nucleon as well as to estimate the structure functions and related quantities [40,41]. On the other hand, the sea quarks dominate for the values of $x < 0.3$. This becomes particularly interesting for the χCQM$_{\text{config}}$ where the effects of sea quarks and effects of valence quarks can separately be calculated. These latest developments have renewed considerable interest in the structure of the light-quark sea as well as valence structure

[a] e-mail: hdahiya@pu.ac.in

of the nucleon and suggests a closer scrutiny of the valence and sea quark distribution functions with an emphasis on their x-dependence.

To predict the quark distributions functions at low and intermediate energy scale, we need to solve the non-perturbative QCD which is an extremely difficult theoretical problem. The question of developing a quark model with confining potential incorporating x-dependence in the valence quarks distribution functions has been discussed in the literature [32–39, 46]. The inclusion of x-dependence however has not yet been successfully derived from first principles. Instead, they are obtained by fitting parametrizations to data. It has also been realized in semiphenomenological analyses [42, 43] that the light flavor sea quark components are absolutely necessary to describe the quark distribution functions. The flavor asymmetry of the sea quark distributions have been established experimentally [9–13] which seems definitely non-perturbative and cannot be explained by the sea quarks radiatively generated through the perturbative QCD. Therefore, some low-energy nonperturbative mechanism is needed which generates sea-quark distributions in the nucleon. Recently, these issues have been discussed in the chiral quark soliton model [44, 45] which makes a reasonable estimation not only of the quark distribution functions but also of the antiquark distributions by taking into account the x-dependence in the distribution functions. More recently, Alwall and Ingelman [47] have derived, in their physical model, the x-dependence in the quark distribution functions from simple assumptions regarding the nonperturbative properties of the hadron. Earlier also, similar kind of calculations have been done by Eichten, Hinchliffe and Quigg in the chiral quark model [15] which describes the sea quark distribution functions. Isgur [32–36] has also discussed the x-dependence of the quark distribution functions, induced by relativistic quenching, in the constituent quark model.

The purpose of the present communication is to phenomenologically include the x-dependence in the valence and sea quark distribution functions in the χCQM$_{\rm config}$ and study its implications for quark flavor asymmetries dominated by the sea quark distribution functions as well as spin independent structure functions dominated by valence quark distribution functions. In particular, we would like to include x-dependence in the quantities which have weak Q^2 dependence, for example, $\bar{d}(x)-\bar{u}(x)$, $\bar{d}(x)/\bar{u}(x)$, $\frac{\bar{d}(x)-\bar{u}(x)}{u(x)-d(x)}$, $F_2^p(x)-F_2^n(x)$ and $F_2^n(x)/F_2^p(x)$. Dependence of the quark distribution functions on x is compared with the data as well as with the results of several theoretical models, for example, the chiral quark soliton model [44, 45], chiral bag model [46], a physical model by Alwall and Ingelman [47], statistical quark model [48] etc. Further, it would also be interesting to carry out a detailed analysis of the implications of configuration mixing in the quantities $F_2^p(x)-F_2^n(x)$ and $F_2^n(x)/F_2^p(x)$, where the valence quarks play an important role. Furthermore, the valence quark structure can also be tested by extrapolating the predictions of our model in the limit $x\to 1$ where data is not available.

2 Chiral constituent quark model with configuration mixing (χCQM$_{\rm config}$)

The details of χCQM$_{\rm config}$ have already been discussed in [23–26], however to facilitate the discussion as well as for the sake of readability of the manuscript, some essential details have been presented in the sequel. The key to understand the "proton spin problem", in the χCQM formalism [16–18], is the fluctuation process

$$q^{\pm}\to {\rm GB}+q'^{\mp}\to (q\bar{q}')+q'^{\mp}\,, \tag{1}$$

where GB represents the Goldstone boson and $q\bar{q}'+q'$ constitute the "quark sea" [16–26]. The effective Lagrangian describing interaction between quarks and a nonet of GBs, consisting of octet and a singlet, can be expressed as

$$\mathcal{L}=g_8\bar{\mathbf{q}}\Phi\mathbf{q}+g_1\bar{\mathbf{q}}\frac{\eta'}{\sqrt{3}}\mathbf{q}=g_8\bar{\mathbf{q}}\left(\Phi+\zeta\frac{\eta'}{\sqrt{3}}I\right)\mathbf{q}=g_8\bar{\mathbf{q}}(\Phi')\mathbf{q}\,, \tag{2}$$

where $\zeta=g_1/g_8$, g_1 and g_8 are the coupling constants for the singlet and octet GBs, respectively, I is the 3×3 identity matrix. The GB field which includes the octet and the singlet GBs is written as

$$\Phi'=\begin{pmatrix}\frac{\pi^0}{\sqrt{2}}+\beta\frac{\eta}{\sqrt{6}}+\zeta\frac{\eta'}{\sqrt{3}} & \pi^+ & \alpha K^+\\ \pi^- & -\frac{\pi^0}{\sqrt{2}}+\beta\frac{\eta}{\sqrt{6}}+\zeta\frac{\eta'}{\sqrt{3}} & \alpha K^0\\ \alpha K^- & \alpha\bar{K}^0 & -\beta\frac{2\eta}{\sqrt{6}}+\zeta\frac{\eta'}{\sqrt{3}}\end{pmatrix}$$

$$\text{and } q=\begin{pmatrix}u\\ d\\ s\end{pmatrix}. \tag{3}$$

SU(3) symmetry breaking is introduced by considering $M_s>M_{u,d}$ as well as by considering the masses of GBs to be nondegenerate ($M_{K,\eta}>M_\pi$) [19–22], whereas the axial U(1) breaking is introduced by $M_{\eta'}>M_{K,\eta}$ [16–22]. The parameter $a(=|g_8|^2)$ denotes the probability of chiral fluctuation $u(d)\to d(u)+\pi^{+(-)}$, whereas $\alpha^2 a$, $\beta^2 a$ and $\zeta^2 a$ respectively denote the probabilities of fluctuations $u(d)\to s+K^{-(0)}$, $u(d,s)\to u(d,s)+\eta$, and $u(d,s)\to u(d,s)+\eta'$.

The most general configuration mixing, generated by the chromodynamic spin–spin forces [31–38], in the case of octet baryons can be expressed as [32–38, 49]

$$\begin{aligned}|B\rangle=&(|56,0^+\rangle_{N=0}\cos\theta+|56,0^+\rangle_{N=2}\sin\theta)\cos\phi\\&+(|70,0^+\rangle_{N=2}\cos\theta'+|70,2^+\rangle_{N=2}\sin\theta')\sin\phi\,,\end{aligned} \tag{4}$$

where ϕ represents the $|56\rangle-|70\rangle$ mixing, θ and θ' respectively correspond to the mixing among $|56,0^+\rangle_{N=0}-|56,0^+\rangle_{N=2}$ states and $|70,0^+\rangle_{N=2}-|70,2^+\rangle_{N=2}$ states. For the present purpose, it is adequate [23–26, 37, 38, 50, 51] to consider the mixing only between $|56,0^+\rangle_{N=0}$ and the $|70,0^+\rangle_{N=2}$ states and the corresponding "mixed" octet of baryons is expressed

$$|B\rangle\equiv\left|8,\tfrac{1}{2}^+\right\rangle=\cos\phi|56,0^+\rangle_{N=0}+\sin\phi|70,0^+\rangle_{N=2}\,, \tag{5}$$

for details of the spin, isospin and spatial parts of the wavefunction, we refer the reader to [52].

3 Quark distribution functions and related parameters

The χCQM$_{\rm config}$ incorporates the valence quarks, the quark sea and the gluons as the effective degrees of freedom. However, there are no simple or straightforward rules which could allow incorporation of x-dependence in χCQM$_{\rm config}$. The kind of parameters we are evaluating in the present context, at the leading order, involve only the valence quarks and the sea quarks and their x-dependence contributing to the total quark distribution functions defined as $q(x) = q_{\rm val}(x) + \bar{q}(x)$ $(q = u, d, s)$. Therefore, we would consider the x-dependence of valence quark distributions given as $u_{\rm val}(x)$, $d_{\rm val}(x)$, $s_{\rm val}(x)$ and the sea quark distributions given as $\bar{u}(x)$, $\bar{d}(x)$, $\bar{s}(x)$. To this end, instead of using an ab initio approach, we have phenomenologically incorporated the x-dependence getting clues from Eichten et al. [15], Isgur [32–36] and Le Yaouanc et al. [37, 38]. To begin with, we emphasize the normalization conditions which have to be satisfied by the quark and antiquarks distribution functions. For example,

$$\begin{aligned}
\int_0^1 [u(x) - \bar{u}(x)]\,{\rm d}x &= \int_0^1 u_{\rm val}(x)\,{\rm d}x = 2\,,\\
\int_0^1 [d(x) - \bar{d}(x)]\,{\rm d}x &= \int_0^1 d_{\rm val}(x)\,{\rm d}x = 1\,,\\
\int_0^1 [s(x) - \bar{s}(x)]\,{\rm d}x &= \int_0^1 s_{\rm val}(x)\,{\rm d}x = 0\,. \qquad (6)
\end{aligned}$$

Keeping in mind the above normalization conditions and following Eichten et al., we assume the x-dependence of the valence and sea quark distribution functions as

$$\begin{aligned}
u_{\rm val}(x) &= 8(1-x)^3\cos^2\phi + 4(1-x)^3\sin^2\phi\\
&\quad + 8\sqrt{2}x^4(1-x)^3\cos\phi\sin\phi\,, \qquad (7)\\
d_{\rm val}(x) &= 4(1-x)^3\cos^2\phi + 2(1-x)^3\sin^2\phi\\
&\quad - 8\sqrt{2}x^4(1-x)^3\cos\phi\sin\phi\,, \qquad (8)\\
\bar{u}(x) &= \frac{a}{12}[(2\zeta+\beta+1)^2+20](1-x)^{10}\,, \qquad (9)\\
\bar{d}(x) &= \frac{a}{12}[(2\zeta+\beta-1)^2+32](1-x)^{7}\,, \qquad (10)\\
\bar{s}(x) &= \frac{a}{3}[(\zeta-\beta)^2+9\alpha^2](1-x)^{8}\,. \qquad (11)
\end{aligned}$$

It should be noted that the effects of configuration mixing have been incorporated in the valence quark distribution functions following Le Yaouanc et al. and Isgur [32–36].

After having formulated the x-dependence in the valence and sea quark distribution functions, we now consider the quantities which are measured at different x and can expressed in terms of the above mentioned quark distribution functions. As mentioned earlier also, we are interested only in the quantities which have weak Q^2 dependence because χCQM does not incorporate Q^2 dependence, therefore we will consider only those experimentally measurable quantities which have no or weak Q^2 dependence. To this end, the most important quantity is the Gottfried integral which can be expressed in terms of the quark distribution functions after separating them into valence and sea contributions and is expressed as

$$\begin{aligned}
I_{\rm G} &= \frac{1}{3}\int_0^1 [u_{\rm val}(x) - d_{\rm val}(x)]\,{\rm d}x + \frac{2}{3}\int_0^1 [\bar{u}(x) - \bar{d}(x)]\,{\rm d}x\\
&= \frac{1}{3} + \frac{2}{3}\int_0^1 [\bar{u}(x) - \bar{d}(x)]\,{\rm d}x\,, \qquad (12)
\end{aligned}$$

where we have used the above normalization conditions. The quantity $\bar{u}(x) - \bar{d}(x)$ can be obtained from the E866 data [11–13] at different x values and calculated in the present context from (9) and (10). Similarly, the $\bar{d}(x)/\bar{u}(x)$ [11–13, 27] asymmetry measured through the ratio of muon pair production cross sections σ_{pn} and σ_{pp}, can expressed in the present case in terms of the sea quark distribution functions and its variation with x can be studied. Further, the x-dependence of $\frac{\bar{d}(x)-\bar{u}(x)}{u(x)-d(x)}$ [28] can be calculated using (7)–(10) as well as the normalization conditions from (6).

To study the Q^2 independent combinations of proton and neutron structure functions $F_2^{p,n}(x, Q^2)$, we write the basic spin independent structure functions in terms of the valence and sea quark distribution functions as follows

$$\begin{aligned}
F_1(x, Q^2) &= \frac{1}{2}\sum_{q=u,d,s} e_q^2[q_{\rm val}(x) + \bar{q}(x)]\,, \qquad (13)\\
F_2(x, Q^2) &= 2xF_1(x, Q^2)\,. \qquad (14)
\end{aligned}$$

The difference of proton and neutron structure functions $F_2^p(x) - F_2^n(x)$ as well as the ratio $R^{np}(x) = F_2^n(x)/F_2^p(x)$ which again have weak Q^2 dependence can be obtained using (7)–(11).

For the strange-quark content of the nucleon, the relevant observables [53–56] measured over a range of x are given as

$$\begin{aligned}
\rho &= 2\frac{\int_0^1 x\bar{s}(x)\,{\rm d}x}{\int_0^1 x(u(x)+d(x))\,{\rm d}x}\,, \qquad (15)\\
\kappa &= 2\frac{\int_0^1 x\bar{s}(x)\,{\rm d}x}{\int_0^1 x(\bar{u}(x)+\bar{d}(x))\,{\rm d}x}\,. \qquad (16)
\end{aligned}$$

The parameters ρ and κ represents the ratio between the strange and nonstrange quarks of the sea. With the ratio ρ/κ we obtain the ratio between the nonstrange antiquarks and quarks in the nucleon as

$$\frac{\rho}{\kappa} = \frac{\int_0^1 x(\bar{u}(x)+\bar{d}(x))\,{\rm d}x}{\int_0^1 x(u(x)+d(x))\,{\rm d}x} \qquad (17)$$

4 Input parameters

Before calculating the valence and sea quark distribution functions and the related phenomenological quantities

such as $\bar{d}(x)-\bar{u}(x)$, $\bar{d}(x)/\bar{u}(x)$, $\frac{\bar{d}(x)-\bar{u}(x)}{u(x)-d(x)}$, $F_2^p(x)-F_2^n(x)$ and $F_2^n(x)/F_2^p(x)$ to study x-dependence, we have to first fix the χCQM$_{\rm config}$ parameters (a, α, β and ζ representing the probabilities of fluctuations to pions, K, η, η') coming in the sea quark distribution functions $\bar{u}(x)$, $\bar{d}(x)$ and $\bar{s}(x)$ as well as the mixing angle ϕ coming in the valence quark distribution functions $u_{\rm val}(x)$ and $d_{\rm val}(x)$. The mixing angle ϕ is fixed from the consideration of neutron charge radius [37, 38, 50, 51], for the other parameters we have used Δu, Δ_3, $\bar{u}-\bar{d}$ and $\bar{u}/\bar{d}$ as inputs. The range of the coupling breaking parameter a can be easily found by considering the spin polarization function Δu, by giving the full variation of parameters α, β and ζ from which one finds $0.10 \le a \le 0.14$. The range of the parameter ζ can be found from $\bar{u}/\bar{d}$ using the latest experimental measurement [11–13] and it comes out to be $-0.70 \le \zeta \le -0.10$. Using the above found ranges of a and ζ as well as the latest measurement of $\bar{u}-\bar{d}$ asymmetry [11–13], β comes out to be in the range $0.2 \le \beta \le 0.7$. Similarly, the range of α can be found by considering the flavor non-singlet component Δ_3 and it comes out to be $0.2 \le \alpha \le 0.5$. After finding the ranges of the coupling breaking parameters, we have carried out a fine grained analysis by fitting Δu, Δd, Δ_3 [64] as well as $\bar{u}-\bar{d}$, $\bar{u}/\bar{d}$ [11–13] leading to the following set of best fit parameters

$$a = 0.13\,, \quad \alpha = \beta = 0.45\,, \quad \zeta = -0.10\,. \qquad (18)$$

Table 1. The calculated values of the spin polarization functions, baryon octet magnetic moments and the quark flavor distribution functions. The value of the mixing angle ϕ is taken to be 20°

Parameter	Data	χCQM$_{\rm config}$ $\zeta=-0.10$ $a=0.13$ $\alpha=0.45$ $\beta=0.45$
Δu^*	0.85 ± 0.05 [3–8]	0.913
Δd	-0.41 ± 0.05 [3–8]	−0.364
Δs	-0.07 ± 0.05 [3–8]	−0.02
$\Delta_3{}^*$	1.267 ± 0.0035 [64]	1.267
Δ_8	0.58 ± 0.025 [64]	0.59
$\Delta\Sigma$	0.19 ± 0.025 [64]	0.27
μ_p	2.79 ± 0.00 [64]	2.81
μ_n	-1.91 ± 0.00 [64]	−1.96
μ_{Σ^-}	-1.16 ± 0.025 [64]	−1.19
μ_{Σ^+}	2.45 ± 0.01 [64]	2.46
μ_{Ξ^o}	-1.25 ± 0.014 [64]	−1.26
μ_{Ξ^-}	-0.65 ± 0.002 [64]	−0.64
$\bar{u}-\bar{d}^*$	-0.118 ± 0.015 [11–13]	−0.117
$\bar{u}/\bar{d}^*$	0.67 ± 0.06 [11–13]	0.67
$I_{\rm G}$	0.254 ± 0.005	0.255
f_3	–	0.209
f_8	–	1.06
f_3/f_8	0.21 ± 0.05 [16–18]	0.20

* input parameters

To check the results in χCQM$_{\rm config}$, we have in Table 1, presented certain parameters related to spin polarization functions and quark distribution functions having implications for the above set of χCQM parameters. The details have already been discussed in [63]. On comparing the results for these quantities with data, it is evident from the table that we are able to obtain an excellent agreement in the case of Δd, Δ_8, baryon octet magnetic moments μ_p, μ_n, μ_{Σ^-}, μ_{Σ^+}, μ_{Ξ^o} and μ_{Ξ^-}. Similar agreement is obtained in the case of quark distribution functions. Therefore, we will be using the above set of χCQM parameters for our calculations.

5 Results and discussion

After having incorporated x-dependence in the valence and sea quark distribution functions as well as fixing the χCQM$_{\rm config}$ parameters, we now discuss all the Q^2 independent quantities at different values of x and compare them with the available experimental data as well as other theoretical models. To begin with, in Figs. 1 and 2, we have shown how the valence and sea quark distributions of the proton vary with the Bjorken scaling variable x. Although no experimental data is available for these quantities, we have plotted them in order to make a comparison with other theoretical results at different x. A cursory look at the plots clearly indicates that our results seem to be well in line with the suggestions of the chiral quark soliton model [44, 45] as well as a physical model by Alwall and Ingelman [47]. In order to compare our results with their results, we can compare the magnitude of quark distribution functions at some particular values of x. For example, in Fig. 1, $xu_{\rm val}(x)$ has a peak at around $x = 0.25$ and the maximum value goes upto 0.9. This is in excellent agreement with the valence quark distribution function in the chiral quark soliton model [44, 45] as well as a physical

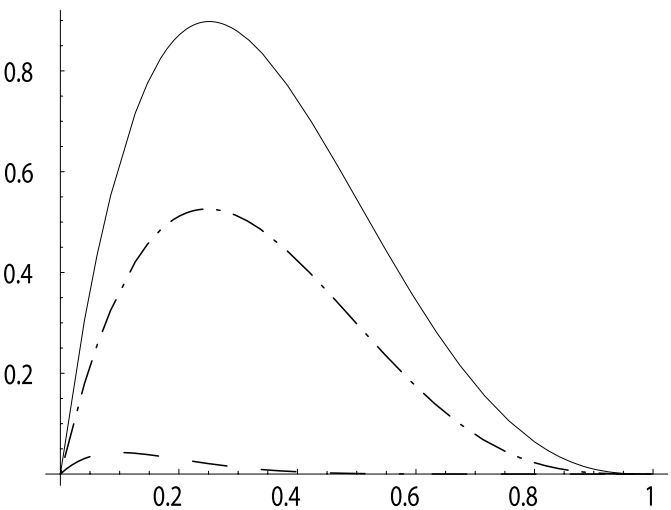

Fig. 1. The variation of valence quark distributions $xu_{\rm val}$ (*solid line*), $xd_{\rm val}$ (*dot-dashed*) and $xs_{\rm val}$ (*dashed*) with the Bjorken scaling variable x

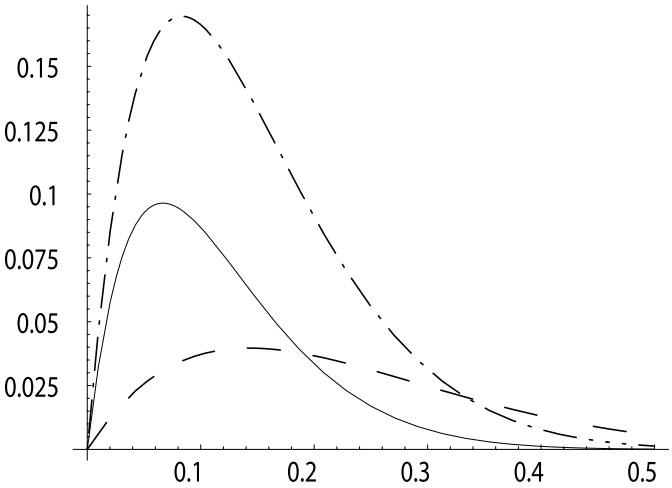

Fig. 2. The variation of sea quark distributions $x\bar{u}$ (*solid line*), $x\bar{d}$ (*dot-dashed*) and $x\bar{s}$ (*dashed*) with the Bjorken scaling variable x

model by Alwall and Ingelman [47]. Similarly, we can compare the sea quark distribution function $x\bar{u}(x)$. In this case also, we find that the peak is at around $x = 0.1$ and the maximum value goes upto 0.1 also in agreement with the above mentioned models. Similar agreement is found from the comparison of the case of $xd_{\rm val}(x)$ and $xs_{\rm val}(x)$ as well as $x\bar{d}(x)$ and $x\bar{s}(x)$.

From these plots, we are also able to describe some general aspects of the valence and sea quark distribution functions. From Figs. 1 and 2, one can easily find out that the valence quark distributions predictions vary as

$$u_{\rm val}(x) > d_{\rm val}(x) > s_{\rm val}(x)\,,$$

whereas the sea quark or the antiquark distributions vary as

$$\bar{d}(x) > \bar{u}(x) > \bar{s}(x)\,.$$

It would be important to mention here that the sea quarks do not contribute at higher values of x, therefore in Fig. 2, we have taken the region $x = 0$–0.5. Beyond this x region the contribution of the sea quarks is negligible. A careful study of the plots brings out several interesting points. It is evident from Fig. 1 that the valence quark distribution is spread over the entire x region and also that there is u quark dominance when $x \to 1$. From Fig. 2, the variation of the magnitudes of $\bar{u}(x)$, $\bar{d}(x)$ and $\bar{s}(x)$ shows that there is an excess of $\bar{d}$ quarks over $\bar{u}$ quarks in the regime where the sea quarks contribute. It is also clear from the plots that as the value of x increases, the sea contributions decrease and when $x > 0.35$, the contributions are completely dominated by the valence quarks. This point would be elaborated further while discussing the $\bar{d}(x) - \bar{u}(x)$ asymmetry which is very much in agreement with the NMC [9, 10] and the more recent E866 asymmetry data [11–13]. A comparison of the valence and sea quark distribution functions also brings out that the contribution of the sea quarks is less than the valence quarks by approximately 10%. These observations are in line with the observations of other models [44–48].

After having discussed some of the general aspects of the variation of the valence and sea quark distribution functions with x, we now discuss the variation of some of the well known experimentally measurable quantities. The variation of the magnitudes of $\bar{u}(x)$, $\bar{d}(x)$ and $\bar{s}(x)$ are of special interest as it explains the $\bar{d}(x) - \bar{u}(x)$ as well as the $\bar{d}(x)/\bar{u}(x)$ asymmetry. A flavor symmetric sea, $\bar{u} = \bar{d}$, leads to the Gottfried sum rule $I_{\rm G} = \frac{1}{3}$. A measurement of the Gottfried integral by NMC [9, 10] and E866 [11–13] has resulted in $I_{\rm G} = 0.235 \pm 0.026$ and 0.254 ± 0.005 respectively. If isospin symmetry holds, a global flavor asymmetry $\int_0^1 (\bar{d}(x) - \bar{u}(x))\,{\rm d}x \approx 0.15$ and 0.12 would account for the NMC and E866 result. It is however interesting to note that the E866 experiment has measured the x-dependence of $\bar{d}(x) - \bar{u}(x)$ and $\bar{d}(x)/\bar{u}(x)$ asymmetries independently and we would henceforth be considering the experiment data of the E866 to compare with the results of our model. In Figs. 3 and 4, the χCQM results for the $\bar{d}(x) - \bar{u}(x)$, $\bar{d}(x)/\bar{u}(x)$ asymmetries are plotted at different x values. A cursory look at the figures shows that the results of our model calculations show a satisfactory overlap with the available E866 data. It would be important to mention that these quantities provide important constrains on a model that attempts to describe the origins of the nucleon sea and has very important implications for the role of sea quarks in the low-x regions. In other words, these asymmetries provide a direct determination of the "quark sea" contribution in the nucleon. It is clear from the plots that when x is small $\bar{d}(x) - \bar{u}(x)$ and $\bar{d}(x)/\bar{u}(x)$ are large implying the dominance of sea quarks in this region. In fact, the sea quarks dominate only in the region where x is smaller than 0.35. On the other hand, when $x \to 1$, $\bar{d} - \bar{u}$ tends to 0 implying that there are no sea quarks in this region because the $\bar{u}$ and $\bar{d}$ quarks are generated from the "quark sea" in χCQM. In this case also,

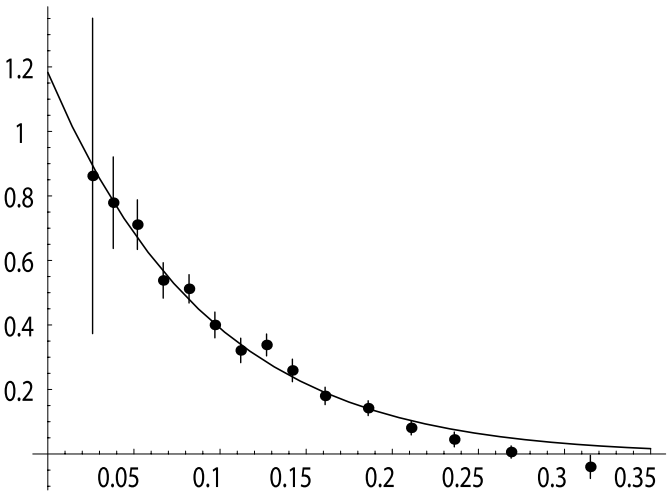

Fig. 3. The variation of $\bar{d}(x) - \bar{u}(x)$ asymmetry with the Bjorken scaling variable x in comparison with the E866 data [11–13] at different x values

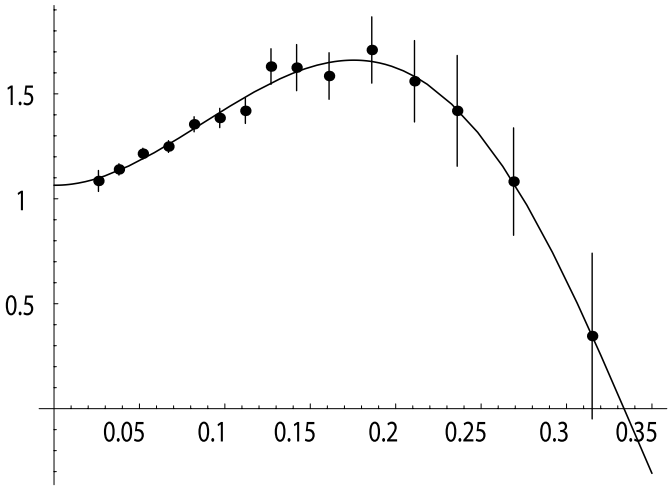

Fig. 4. The variation of $\bar{d}(x)/\bar{u}(x)$ asymmetry with the Bjorken scaling variable x in comparison with the E866 data [11–13] at different x values

our results are well in agreement with the other theoretical results [44–48].

In Fig. 5, we have plotted the phenomenological results for the $\frac{\bar{d}(x)-\bar{u}(x)}{u(x)-d(x)}$ asymmetry at different values of x and have compared them with the available semi-inclusive DIS experimental data [28]. The values of $\frac{\bar{d}(x)-\bar{u}(x)}{u(x)-d(x)}$ are positive over the region $0.02 < x < 0.35$ again showing an excess of $\bar{d}$ over $\bar{u}$. It is also evident from the plot that more experimental input is required for the quantity to be compared with the predictions of the model as the error contained in the data is too large. Therefore, a refinement in the data would not only test the x-dependence in the quark distribution functions but also the extent to which the quark sea contributes in the low-x regime.

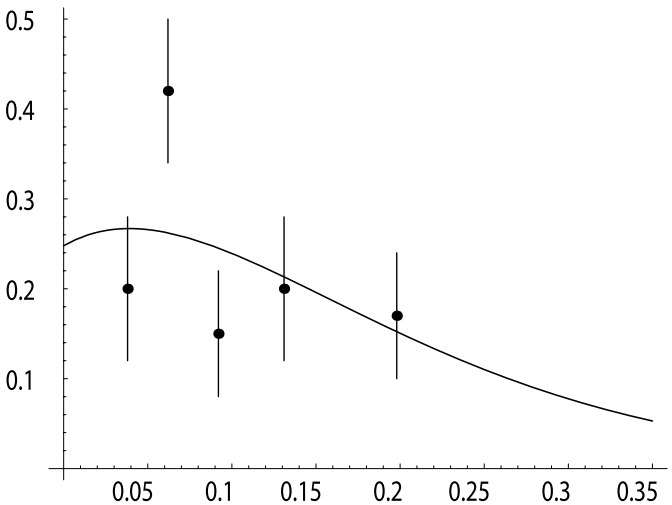

Fig. 5. The variation of $\frac{\bar{d}(x)-\bar{u}(x)}{u(x)-d(x)}$ asymmetry with the Bjorken scaling variable x in comparison with the HERMES data [28] at different x values

The above mentioned quantities test the sea quark distributions, dominant in the low-x regime, reasonably well. It would be important to mention here that the results presented here depend mainly on the χCQM parameters. However, to test the inclusion of x-dependence in the high-x regime, it becomes essential to study the valence quark distributions which play an important role in the proton and neutron structure functions and in this case the results depend mainly on the assumed parameterization of the x-shape. In Figs. 6 and 7, we have plotted the phenomenological results for the difference and the ratio of the structure functions ($F_2^p(x) - F_2^n(x)$ and $R^{np} = F_2^n(x)/F_2^p(x)$) after the inclusion of configuration mixing and have compared them with the available data [30]. A cursory look at

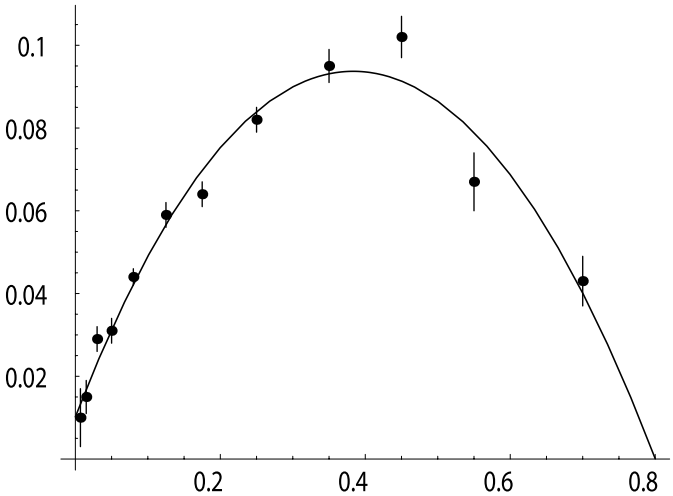

Fig. 6. The variation of the difference of proton and neutron structure functions $F_2^p(x) - F_2^n(x)$ with the Bjorken scaling variable x in comparison with the NMC data [30] at different x values

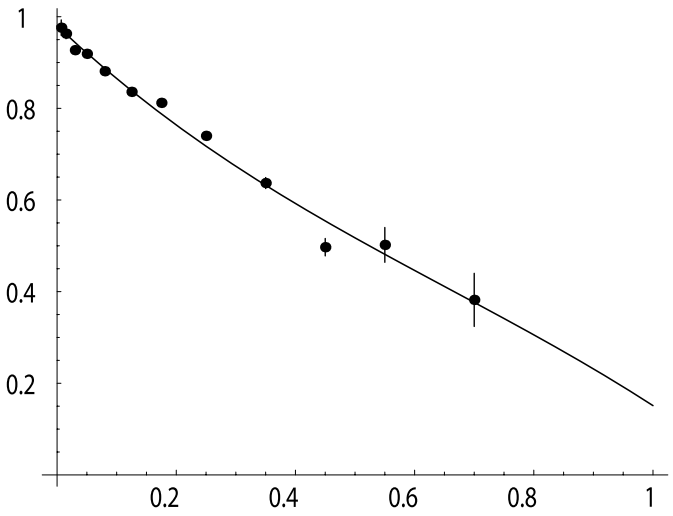

Fig. 7. The variation of the ratio of neutron and proton structure functions $R^{np}(x) = \frac{F_2^n(x)}{F_2^p(x)}$ with the Bjorken scaling variable x in comparison with the NMC data [30] at different x values

the plots immediately brings out that our phenomenological results have a very good overlap with the data. To make a comparison at some particular values of x, in Table 2, we have also presented the results for $F_2^p(x) - F_2^n(x)$ and $F_2^n(x)/F_2^p(x)$ at different values of x. A careful scrutiny of the plots and the table reveals several important points. As the data in the case of the above mentioned structure functions is available for a broader range of x as compared to the data available for the sea quark asymmetries therefore, it becomes interesting to highlight the importance of valence and sea quarks in different x regimes. We have carried out a detailed analysis for the valence and sea quark contribution to $F_2^p(x) - F_2^n(x)$ and it is found that in the low-x regime the contributions are dominated by sea quarks whereas, as we go to higher x values the contributions are completely dominated by the valence quarks. It is however interesting to note that the valence and sea quark distributions contribute in the right direction to give an excellent overall fit to $F_2^p(x) - F_2^n(x)$.

Similarly in the case of R^{np}, the agreement of our phenomenological results with the data are excellent over the entire x range. In this case also the valence and sea quark distributions contribute in the right direction for the entire x range. As there is no data available for $x > 0.7$, it therefore becomes more interesting to predict the values at $x \to 1$ and determine the valence structure of the nucleon. Experimentally, R^{np} decreases monotonically with the Bjorken scaling variable x from $R^{np} \simeq 1$ at $x \simeq 0$ to $R^{np} \simeq \frac{1}{3}$ at $x \simeq 0.7$. In our model we predict

$$R^{np}(x = 0.05) = 0.920\,,$$
$$R^{np}(x = 1) = 0.238\,, \qquad (19)$$

apart from the values at different x. The results compare extremelly well with the experimental figures. Our results are also in line with other theoretical models such as the chiral quark soliton model [44, 45], statistical quark model [48] as well as a physical model by Alwall and Ingelman [47] particularly when the value of x is small. However, when we go to higher values of x, our model predictions are in better agreement with data when compared to the above mentioned theoretical models. This can easily be seen by comparing the plots of these models with our predictions.

As has been mentioned earlier, the inclusion of configuration mixing generated by spin-spin forces [31–38] in the naive constituent quark model provides a natural explanation for many of the nucleon properties including the behaviour of the difference and the ratio of the structure functions $F_2^p(x) - F_2^n(x)$ and $F_2^n(x)/F_2^p(x)$ as $x \to 1$ where the valence quarks play a dominant role. Therefore, to emphasize the importance of configuration mixing, we have have also carried out the calculations without configuration mixing and presented them in Table 2. In order to appreciate the role of x-dependence along with configuration mixing, we first compare the results of the χCQM with those of the χCQM$_{\rm config}$. We find that the configuration mixing effects a uniform improvement in the case of structure functions compared to those without configuration mixing. We also find that the inclusion of x in the quark distribution functions predicts the results in the right direction even when configuration mixing is not included, however, when configuration mixing is included, these show considerable further improvement. This indicates that both x-dependence and configuration mixing are very much needed to get an overall fit.

To test the validity of the model as well as for the sake of completeness, in Table 3, we have presented the results of our calculations for the quantities whose data is available over a range of x or at an average value of x. In these quantities also we find a good overall agreement with the data. We have already discussed the excellent agreement achieved in the case of $\bar{d}(x) - \bar{u}(x)$ asymmetry at different values of x. The data for this quantity is also available for the ranges $x = 0$–1 and $x = 0.05$–

Table 2. The calculated values of the $F_2^p(x) - F_2^n(x)$ and $\frac{F_2^n(x)}{F_2^p(x)}$ in χCQM and χCQM$_{\rm config}$ at different values of x

	$F_2^p(x) - F_2^n(x)$			$R^{np}(x) = \frac{F_2^n(x)}{F_2^p(x)}$		
$\langle x \rangle$	Data	χCQM	χCQM$_{\rm config}$	Data	χCQM	χCQM$_{\rm config}$
0.007	0.010 ± 0.007	0.028	0.013	0.976 ± 0.017	1.294	0.971
0.015	0.015 ± 0.004	0.054	0.017	0.963 ± 0.011	1.241	0.962
0.030	0.029 ± 0.003	0.053	0.023	0.927 ± 0.007	1.258	0.943
0.050	0.031 ± 0.003	0.063	0.031	0.919 ± 0.007	1.228	0.920
0.080	0.044 ± 0.002	0.073	0.042	0.881 ± 0.006	1.217	0.886
0.125	0.059 ± 0.003	0.085	0.057	0.836 ± 0.007	1.170	0.838
0.175	0.064 ± 0.003	0.098	0.069	0.812 ± 0.009	1.120	0.788
0.250	0.082 ± 0.003	0.106	0.084	0.740 ± 0.008	1.045	0.717
0.350	0.095 ± 0.004	0.112	0.093	0.637 ± 0.012	0.955	0.632
0.450	0.102 ± 0.005	0.110	0.091	0.497 ± 0.019	0.884	0.554
0.550	0.067 ± 0.007	0.102	0.078	0.502 ± 0.038	0.814	0.481
0.700	0.043 ± 0.006	0.058	0.040	0.382 ± 0.058	0.712	0.376
0.800	–	0.046	0.022	–	0.626	0.293
0.900	–	0.033	0.016	–	0.602	0.259
1	–	0.021	0.008	–	0.323	0.239

Table 3. The calculated values of the $\bar{d}(x)-\bar{u}(x)$ asymmetry, $\bar{d}(x)-\bar{u}(x)$, ρ and κ over a range of x

Quantity	x range	Data	χCQM$_{\rm config}$
$\int(\bar{d}(x)-\bar{u}(x))\,\mathrm{d}x$	0–1	0.118 ± 0.012	0.117
$\int(\bar{d}(x)-\bar{u}(x))\,\mathrm{d}x$	0.05–0.35	0.0803 ± 0.011	0.08
$\rho=2\frac{\int_0^1 xs(x)\,\mathrm{d}x}{\int_0^1 x(u(x)+d(x))\,\mathrm{d}x}$	0–1	$0.099^{+0.009}_{-0.006}$	0.09
$\kappa=2\frac{\int_0^1 xs(x)\,\mathrm{d}x}{\int_0^1 x(\bar{u}(x)+\bar{d}(x))\,\mathrm{d}x}$	0–1	$0.477^{+0.063}_{-0.053}$	0.47
$\frac{\rho}{\kappa}=\frac{\int_0^1 x(\bar{u}(x)+\bar{d}(x))\,\mathrm{d}x}{\int_0^1 x(u(x)+d(x))\,\mathrm{d}x}$	0–1	0.2075	0.191

0.35 and is given as $\int_0^1(\bar{d}(x)-\bar{u}(x))\,\mathrm{d}x=0.118\pm0.012$ and $\int_{0.05}^{0.35}(\bar{d}(x)-\bar{u}(x))\,\mathrm{d}x=0.0803\pm0.011$. We find that, in our model, we are also able to give an almost perfect fit for the data available at these x ranges. It also needs to be mentioned that the data for the strangeness dependent parameters mentioned in (15) and (16) is also available for the range $x=0$–1. These quantities lead to some important observations. As there are no strange quarks in the valence structure of the nucleon, therefore the valence contribution to the strangeness parameters ρ and κ is zero. This implies that the contribution is purely from the quark sea. The quality of numerical agreement in this case can be assessed only after the data gets refined.

6 Summary and conclusions

To summarize, in order to enlarge the scope of χCQM$_{\rm config}$, we have phenomenologically incorporated the x-dependence in the quark distribution functions following Le Yaouanc et al. and Eichten et al. After having calculated valence and sea quark distributions $q_{\rm val}(x)$ and $\bar{q}(x)$, we have carried out a detailed analysis to estimate $\bar{d}(x)-\bar{u}(x)$, $\bar{d}(x)/\bar{u}(x)$, $\frac{\bar{d}(x)-\bar{u}(x)}{u(x)-d(x)}$, $F_2^p(x)-F_2^n(x)$ and $F_2^n(x)/F_2^p(x)$ as functions of x where we are able to achieve an excellent agreement with data as well as other theoretical studies for all the quantities simultaneously. Implications of configuration mixing have also been studied and it is found that the inclusion of x predicts the results in the right direction even when configuration mixing is not included, however, when configuration mixing is included, these show considerable further improvement. The valence quark structure has also been tested by extrapolating the predictions of our model in the region $x\to1$ where data is not available. The strangeness dependent parameters ρ and κ coming purely from the sea degrees of freedom leads to some important observations regarding the dependence of the sea quark distibution functions on the Bjorken scale variable x which can perhaps be substantiated by further refinement in the data.

Acknowledgements. H.D. would like to thank DST (Fast Track Scheme), Government of India, for financial support and the chairman, Department of Physics, for providing facilities to work in the department.

References

1. S. Weinberg, Physica A **96**, 327 (1979)
2. A. Manohar, H. Georgi, Nucl. Phys. B **234**, 189 (1984)
3. EMC Collaboration, J. Ashman et al., Phys. Lett. B **206**, 364 (1988)
4. EMC Collaboration, J. Ashman et al., Nucl. Phys. B **328**, 1 (1989)
5. SMC Collaboration, B. Adeva et al., Phys. Lett. B **302**, 533 (1993)
6. P. Adams et al., Phys. Rev. D **56**, 5330 (1997)
7. E142 Collaboration, P.L. Anthony et al., Phys. Rev. Lett. **71**, 959 (1993)
8. E143 Collaboration, K. Abe et al., Phys. Rev. Lett. **75**, 391 (1995)
9. New Muon Collaboration, P. Amaudruz et al., Phys. Rev. Lett. **66**, 2712 (1991)
10. M. Arneodo et al., Phys. Rev. D **50**, R1 (1994)
11. E866/NuSea Collaboration, E.A. Hawker et al., Phys. Rev. Lett. **80**, 3715 (1998)
12. J.C. Peng et al., Phys. Rev. D **58**, 092 004 (1998)
13. R.S. Towell et al., Phys. Rev. D **64**, 052 002 (2001)
14. K. Gottfried, Phys. Rev. Lett. **18**, 1174 (1967)
15. E.J. Eichten, I. Hinchliffe, C. Quigg, Phys. Rev. D **45**, 2269 (1992)
16. T.P. Cheng, L.F. Li, Phys. Rev. Lett. **74**, 2872 (1995)
17. T.P. Cheng, L.F. Li, hep-ph/9709293
18. T.P. Cheng, L.F. Li, Phys. Rev. D **57**, 344 (1998)
19. X. Song, J.S. McCarthy, H.J. Weber, Phys. Rev. D **55**, 2624 (1997)
20. X. Song, Phys. Rev. D **57**, 4114 (1998)
21. J. Linde, T. Ohlsson, H. Snellman, Phys. Rev. D **57**, 452 (1998)
22. T. Ohlsson, H. Snellman, Eur. Phys. J. C **7**, 501 (1999)
23. H. Dahiya, M. Gupta, Phys. Rev. D **64**, 014 013 (2001)
24. H. Dahiya, M. Gupta, Phys. Rev. D **66**, 051 501 (2002)
25. H. Dahiya, M. Gupta, Phys. Rev. D **67**, 074 001 (2003)
26. H. Dahiya, M. Gupta, Phys. Rev. **67**, 114 015 (2003)
27. NA51 Collaboration, A. Baldit et al., Phys. Lett. B **253**, 252 (1994)
28. HERMES Collaboration, K. Ackerstaff et al., Phys. Rev. Lett. **81**, 5519 (1998)
29. J.J. Aubert et al., Nucl. Phys. B **293**, 740 (1987)
30. M. Arneodo et al., Phys. Rev. D **50**, R1 (1994)
31. A. De Rujula, H. Georgi, S.L. Glashow, Phys. Rev. D **12**, 147 (1975)
32. N. Isgur, G. Karl, R. Koniuk, Phys. Rev. Lett. **41**, 1269 (1978)

33. N. Isgur, G. Karl, Phys. Rev. D **21**, 3175 (1980)
34. N. Isgur et al., Phys. Rev. D **35**, 1665 (1987)
35. P. Geiger, N. Isgur, Phys. Rev. D **55**, 299 (1997)
36. N. Isgur, Phys. Rev. D **59**, 034013 (1999)
37. A. Le Yaouanc, L. Oliver, O. Pene, J.C. Raynal, Phys. Rev. D **12**, 2137 (1975)
38. A. Le Yaouanc, L. Oliver, O. Pene, J.C. Raynal, Phys. Rev. D **15**, 844 (1977)
39. M. Gupta, A.N. Mitra, Phys. Rev. D **18**, 1585 (1978)
40. CDHS Collaboration, H. Abramowicz et al., Z. Phys. C **17**, 283 (1983)
41. Costa et al., Nucl. Phys. B **297**, 244 (1988)
42. M. Glück, E. Reya, A. Vogt, Z. Phys. C **67**, 433 (1995)
43. M. Glück, E. Reya, M. Stratmann, W. Vogelsang, Phys. Rev. D **53**, 4775 (1996)
44. H. Weigel, Phys. Rev. D **55**, 6910 (1997)
45. M. Wakamatsu, Phys. Rev. D **67**, 034005 (2003)
46. A.I. Signal, A.W. Thomas, Phys. Rev. D **40**, 2832 (1989)
47. J. Alwall, G. Ingelman, Phys. Rev. D **71**, 094015 (2005)
48. L.A. Trevisan, T. Frederico, L. Tomio, Eur. Phys. J. C **11**, 351 (1999)
49. P.N. Pandit, M.P. Khanna, M. Gupta, J. Phys. G **11**, 683 (1985)
50. M. Gupta, N. Kaur, Phys. Rev. D **28**, 534 (1983)
51. M. Gupta, J. Phys. G: Nucl. Part. Phys. **16**, L213 (1990)
52. A. Le Yaouanc et al., Hadron Transitions in the Quark Model (Gordon and Breach, New York, 1988)
53. J. Grasser, H. Leutwyler, M.E. Saino, Phys. Lett. B **253**, 252 (1991)
54. A.O. Bazarko et al., Z. Phys. C **65**, 189 (1995)
55. S.J. Dong, J.F. Lagae, K.F. Liu, Phys. Rev. Lett. **75**, 2096 (1995)
56. M. Goncharov et al., Phys. Rev. D **64**, 112006 (2001)
57. J.D. Bjorken, Phys. Rev. **148**, 1467 (1966)
58. J.D. Bjorken, Phys. Rev. D **1**, 1376 (1970)
59. J. Ellis, R.L. Jaffe, Phys. Rev. D **9**, 1444 (1974)
60. J. Ellis, R.L. Jaffe, Phys. Rev. **10**, 1669 (1974)
61. M. Gupta, A.N. Mitra, Phys. Rev. D **18**, 1585 (1978)
62. N. Isgur, G. Karl, D.W.L. Sprung, Phys. Rev. **23**, 163 (1981)
63. H. Dahiya, M. Gupta, J.M.S. Rana, Int. J. Mod. Phys. A **21**, 4255 (2006)
64. W.-M. Yao et al., J. Phys. G **33**, 1 (2006)